Optimizing Concrete Retaining Wall Design: A Parametric Study on Soil Friction and Toe-to-Heel Ratio

Riza Suwondo
Civil Engineering Department, Faculty of Engineering, Bina Nusantara University, Jakarta, 11480, Indonesia
riza.suwondo@binus.ac.id (corresponding author)

Militia Keintjem
Civil Engineering Department, Faculty of Engineering, Bina Nusantara University, Jakarta, 11480, Indonesia
militia.marchella@binus.ac.id

Aksan Kawanda
Faculty of Civil Engineering and Planning, Universitas Trisakti, Jakarta, Indonesia
aksan.kawanda@trisakti.ac.id

Received: 22 June 2025 | Revised: 25 July 2025 | Accepted: 14 August 2025

 DOI: https://doi.org/10.48084/etasr.12873

ABSTRACT

Concrete Retaining Walls (CRWs) remain the most widely used system for stabilizing the earth slopes; however, their safety margins depend on both the soil properties and base geometry. Although numerous analytical and numerical studies have been conducted, the combined influence of the backfill shear strength and Toe-to-Heel (T:H) proportioning on the global stability has not been quantified across the height range, typical of transportation and infrastructure projects. This study addresses this gap by evaluating how the backfill friction angle and T:H affect the Factors of Safety (FS) against sliding, overturning, and bearing-capacity failure for walls 4 m to 10 m in height. A series of wall configurations was analyzed using closed-form limit-equilibrium equations that incorporate Rankine active earth pressure and eccentric footing stresses. The results show that increasing the backfill friction angle lowers the active pressure coefficient nonlinearly, increasing the sliding and overturning factors by up to 150% for 10 m walls and postponing the bearing failure by approximately 2 m in height. Extending the heel (T:H ≈ 0.5) provides up to a two-fold increase in the sliding and overturning resistance relative to a toe-dominant base, whereas lengthening the toe alone produces only marginal gains and has little impact on the bearing safety. Thus, the current study provides quantitative guidance that enables designers to trade off the soil quality and geometric proportions for a safer and more economically retaining wall construction.

Keywords-component; formatting; style; styling; insert

I. INTRODUCTION

CRWs are among the most widely used solutions for resisting the lateral earth pressures. They support the soil on hillsides, agricultural terraces, roadway embankments, and riverbanks, and carry the surcharge loads imposed on the ground surfaces. Designing an effective CRW begins with a reliable estimate of the lateral loads and a thorough assessment of the stability against sliding, overturning, and bearing-capacity failure [1-4]. These checks depend on the shear strength parameters and unit weights of both the in situ and embankment soils. Because the lateral earth pressure constitutes the dominant loading on the wall, an accurate quantification, whether by Coulomb–Rankine theories or more advanced earth-pressure models, remains a central task in the wall analysis and design [5-7]. Engineers follow an iterative two-stage procedure in routine practice. They first select the trial wall dimensions and verify the geotechnical stability (sliding, overturning, eccentricity, and allowable bearing pressure) using conventional limit equilibrium equations. Finite-element analyses are sometimes performed to capture the deformation patterns and global failure mechanisms [8-12]. Once a trial section satisfies all soil-structure interaction criteria, reinforcement detailing is performed to meet the

structural demands in the stem, heel, and toe. Because this sequential process relies heavily on the designer experience, it seldom guarantees a cost-optimal solution, and can obscure the relative influence of the soil parameters, surcharge position, or base geometry on the overall safety. To overcome the limitations of manual trial-and-error design, researchers began to apply optimization techniques more than four decades ago. Authors in [13] pioneered this approach, and authors in [14] formulated the CRW design as a constrained nonlinear programming problem with seven geometric and reinforcement variables and ten potential failure modes: overturning, sliding, eccentricity, bearing pressure, plus shear and bending in the toe slab, heel slab, and stem. Since then, numerous studies have refined the objective functions, constraint sets, and solution algorithms to produce more economical and reliable retaining wall designs while satisfying all stability requirements.

Authors in [15] improved the classical earth-pressure theory by introducing a double-failure-surface model for CRWs, which better reflects the progressive failure mechanisms observed in practice. However, the overall stability of a CRW depends on many factors beyond the earth pressure alone, including the foundation stiffness and strength, wall geometry, surcharge position, and seepage conditions, variables that conventional limit-equilibrium methods often cannot fully capture. To address these complexities, researchers have increasingly used Finite Element (FE) modeling, with studies such as [16–18] examining the wall deformation and stress paths under both static and seismic loading. Beyond displacement-based FE approaches, Finite-Element Limit Analysis (FELA) combined with the strength-reduction method constitute a robust tool for assessing the global stability, as demonstrated in [19–21]. Despite these advances, systematic parametric evaluations that simultaneously consider the wall geometry, T:H ratios, soil variability, and surcharge effects remain limited. In particular, the combined influence of the T:H ratio, which governs the weight distribution, overturning resistance, and the backfill friction angle, which controls the active earth pressure, has not been comprehensively quantified across realistic wall heights. As a result, the current design guidance continues to rely on fixed geometric rules or isolated parameter studies, restricting the opportunities for rigorous optimization. The present study addresses this gap by examining the stability of reinforced-concrete cantilever retaining walls under varying backfill friction angles and T:H ratios. The stability is assessed for three governing failure modes: sliding, overturning, and bearing capacity. The findings aim to provide practical design insights, enabling engineers to make more informed choices about the wall geometry and soil properties during both the preliminary and detailed design stages.

II. METHODOLOGY

This study investigated the stability performance of reinforced-concrete cantilever retaining walls under varying geometric and soil conditions. The analysis focused on three key failure modes: sliding, overturning, and bearing capacity. A parametric approach was employed to assess how different T:H ratios, backfill friction angles, and wall heights affected the overall safety and performance of the wall. The geometric configuration of the cantilever wall analyzed in this study is shown in Figure 1. The wall consists of a vertical stem with a uniform thickness of 0.4 m and a base slab of the same thickness. The total width of the base slab was fixed at 4 m. Excluding the stem thickness, the remaining 3.6 m of the base was divided between the toe and heel, and their proportions were controlled by the T:H ratio. The wall height was varied from 4 m to 10 m to represent a range of practical applications, from low retaining walls used in landscaping to taller walls used in infrastructure projects.

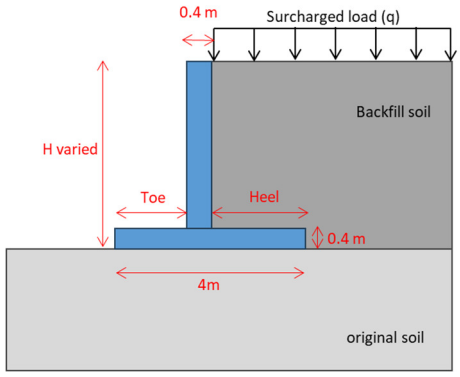

Fig. 1. Cantilever wall configuration.

Two types of soil were considered in the analysis: the original foundation soil and backfill soil. The original soil beneath the wall footing was assumed to be a compacted residual or lightly cemented silty sand with a cohesion of 20 kPa, a friction angle of 35°, and a unit weight of 18 kN/m³. The backfill soil was considered cohesionless with a unit weight of 19 kN/m³. Three backfill friction angles were examined to represent different compaction levels: 25°, 35°, and 45°, corresponding to lose, medium-dense, and dense granular soils, respectively. The unit weight of concrete was assumed to be 25 kN/m³. In addition to the self-weight of the wall and retained soil, a uniform external surcharge of 10 kN/m² was applied to the backfill surface to simulate the traffic, storage, or structural loading. The analysis assumed a level backfill surface, dry soil conditions (no groundwater), and no wall-soil interface friction. This parametric study was conducted in two stages. In the first stage, the backfill friction angle varied at 25°, 35°, and 45° while maintaining a fixed T:H ratio of 1. In the second stage, the T:H ratio varied between 0.5, 1, and 2, with the backfill friction angle held constant at 35°. Each parameter set was analyzed for wall heights ranging from 4 m to 10 m.

After the geometry and material properties had been defined for each parametric case, the wall was checked for three limit states, sliding, overturning, and bearing-capacity failure, using closed-form limit equilibrium expressions. The calculations adopted the Rankine active-pressure theory [22], a dry backfill, and zero interface friction. Consequently, the horizontal earth thrust Pa acting at a height of *H/3* above the base is:

$$P_a = \frac{1}{2} K_a \gamma H^2 + K_a q H \quad (1)$$

$$K_a = tan^2\left(45° - \frac{\varphi}{2}\right) \quad (2)$$

where K_a denotes the Rankine active coefficient, γ denotes the backfill unit weight, q denotes the surcharge, and H denotes the wall height.

The safety factor against sliding (FS_{SL}) compares the available resisting force (base friction) to the driving horizontal thrust:

$$FS_{SL} = \frac{\mu \sum W}{P_a} \quad (3)$$

where μ is the base friction coefficient (taken as tan ϕ = tan 35º for the original foundation soil), and ΣW is the total vertical load on the base.

The overturning moment (M_{OT}) is generated by the horizontal earth pressure and the component of the surcharge:

$$M_{OT} = P_a \frac{H}{3} \quad (4)$$

The resisting moment (M_R) was provided by the vertical force acting on the toe:

$$M_R = W_c x_c + W_b x_b + (qB)x_q \quad (5)$$

where x_c, x_b, and x_q are the lever arms to the toe. The FS becomes:

$$FS_{OT} = \frac{M_R}{M_{OT}} \quad (6)$$

The eccentricity of the resultant vertical load is obtained from:

$$e = \frac{M_R - M_{OT}}{\sum W} \quad (7)$$

which is subsequently used in the bearing capacity check.

Assuming a rigid base and linear stress distribution, the contact pressures beneath the footing (σ) are calculated by:

$$\sigma = \frac{\sum W}{B}\left(1 \pm \frac{6e}{B}\right) \quad (8)$$

The FS for the bearing capacity failure is:

$$FS_{BC} = \frac{\sigma_u}{\sigma} \quad (9)$$

where σ_{ult} is the ultimate bearing capacity computed using the Terzaghi bearing capacity theory [17] for shallow foundations resting on cohesive-frictional soils (c–ϕ soils), assuming a strip footing condition. The general form of the equation is:

$$\sigma_{ult} = cN_c + \gamma D_f N_q + 0.5\gamma B N_\gamma \quad (10)$$

where c is the cohesion of the foundation soil, γ is unit weight of the foundation soil, D_f is depth of the wall footing (assumed equal to the wall base thickness, 0.4 m), B is width of the wall footing (4 m), and N_c, N_q, N_γ are the bearing capacity factors, which are functions of the friction angle ϕ of the foundation soil.

The analytical procedure was systematically applied to each wall configuration defined in the parametric study. For every combination of the wall height, backfill friction angle, and T:H ratio, the corresponding FS against sliding, overturning, and bearing capacity failure are computed. The results are then synthesized to establish stability envelopes and to identify the optimal geometric proportions, particularly T:H ratios that ensure a safe and efficient retaining wall design under varying soil and height conditions.

III. RESULTS AND DISCUSSION

A. Influence of Backfill Friction Angle on Wall Stability

The backfill friction angle (ϕ) plays a fundamental role in determining the lateral earth pressure exerted on retaining structures, thereby influencing their overall stability. In this study, the effect of ϕ was investigated across three representative values (25°, 35°, and 45°) while keeping the T:H ratio fixed at 1. These values reflect the conditions ranging from loose to dense granular soils, commonly encountered in retaining wall applications. For each friction angle, wall heights ranging from 4 to 10 m were analyzed. The evaluation focuses on the FS against sliding, overturning, and bearing capacity failure to assess how increasing the soil shear strength affects the structural performance. A comparative analysis of the FS for the three governing limit states (sliding, overturning, and bearing capacity) across the three different backfill friction angles is presented in Figure 2. The sliding factor of the safety curve (Figure 2(a)) confirms the quadratic sensitivity of the active earth thrust to the wall height: FS declines steadily as H increases for every friction angle examined. At any given height, a larger ϕ yielded a markedly higher FS because the Rankine coefficient (K_a) decreased nonlinearly with increasing shear strength. The divergence between the three curves widened with height, indicating that backfill improvement provided the greatest benefit for tall walls. When ϕ = 25°, the FS falls below the conventional target value of 1.5 when the wall exceeds approximately 6 m. For ϕ = 35°, the same threshold is not reached until approximately 9 m. At ϕ = 45°, the sliding remained acceptable to the upper bound of the study (10 m). Hence, for walls taller than 6 m–7 m, dense granular backfills or auxiliary shear-resistance measures are essential to prevent sliding. The overturning results shown in Figure 2(b) display a consistent decline in the FS with an increasing wall height, like the sliding trend. However, the overturning FS are generally higher than those for sliding due to the stabilizing moment contributed by the wall and backfill weight, which increases linearly with height, while the overturning moment grows quadratically. For ϕ = 25°, the FS falls below the conventional threshold of 1.5 at a height of approximately 7 m. When the backfill friction angle was increased to ϕ = 35°, the wall could safely reach approximately 9 m before exceeding the critical threshold. With ϕ = 45°, the overturning FS remains above 1.5 for all evaluated wall heights. The widening separation between the 25° and 45° curves at greater heights further highlights the advantage of using high friction backfill materials to enhance the overturning resistance by reducing the active pressure and improving the eccentricity control. As the slab thickness increased beyond 200 mm, the bearing capacity FS, as shown in Figure 2 (c), was an order of magnitude higher than that for sliding and overturning at low wall heights because the resultant remained close to the base center, producing low stress intensities relative to the allowable pressure (calculated with a global FS = 3).

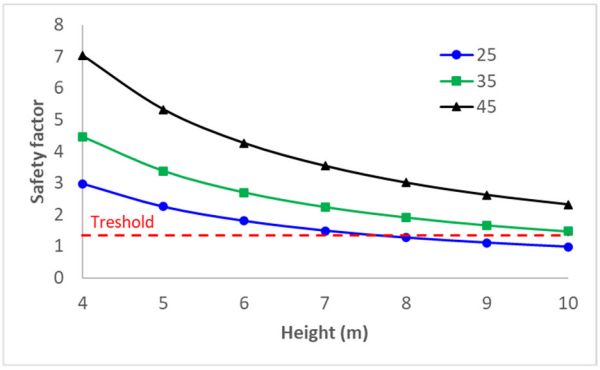

a. Sliding

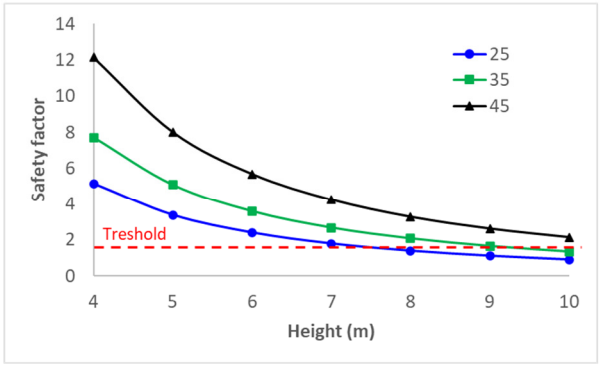

b. Overturning

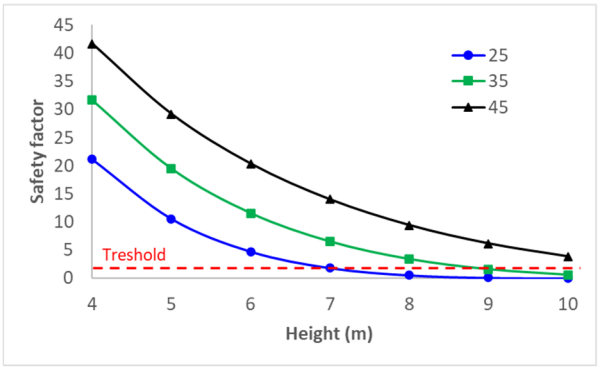

c. Bearing capacity

Fig. 2. Effect of backfill friction angle on Stability of cantilever retaining walls.

However, the bearing safety deteriorates far more rapidly with height than the other two modes, reflecting the cubic influence of eccentricity on σ_{max}. For the poorest backfill (ϕ = 25°), the FS dropped below the target value of 3 at approximately 7 m and approached unity at 9 m–10 m, indicating imminent bearing failure. With ϕ = 35°, the 3 threshold is crossed near 8 m, while with ϕ = 45°, an adequate margin is retained through 9 m, falling marginally below 3 only at 10 m. Thus, the bearing pressure becomes the governing limit state for walls higher than ~7 m, unless the heel length is increased or foundation improvement is undertaken. The results emphasize the significant advantage of using higher-friction backfill, particularly for walls taller than 7 m. Increasing the backfill friction angle from 25° to 35° extends the allowable wall height by about 2 m before any failure mode becomes critical, while raising it further to 45° adds another 1 m–2 m of safe height. The benefits are most pronounced for sliding and overturning: for a 10 m wall, increasing ϕ from 25° to 45° improves the sliding FS from roughly 0.9 to 2.3 and the overturning factor from about 1 to 2.5, an increase of more than 150%. These findings highlight the importance of specifying high-quality backfill in tall wall design. If such a material is unavailable, the designers should take additional resistance measures (e.g., shear keys, counterforts, or ground reinforcement) and pay closer attention to the bearing-capacity checks than those typically required for shorter walls.

B. Influence of T:H Ratio on Wall Stability

In the second part of the parametric study, the backfill friction angle was fixed at 35º, which is representative of well-compacted granular soil, whereas the T∶H ratio of the base slab was varied between 0.5, 1, and 2. These values span the practical range from a relatively short heel (economical but potentially unstable) to an extended heel that maximizes the stabilizing weight and moment. Figure 3 plots the FS for sliding, overturning, and bearing capacity as functions of a wall height between 4 m and 10 m. The sliding results, as depicted in Figure 3 (a), demonstrate that a larger heel increases both the stabilizing weight on the base and the moment arm of that weight, thereby increasing the frictional resistance against lateral thrust. At H = 4 m, the long-heel wall (T:H = 0.5) achieved a sliding FS of approximately 8, which is more than double that of the short-heel wall (T:H = 2). Although the advantage diminishes with height, the T:H = 0.5 configuration remains the only one to satisfy the target FS ≥ 1.5 at H = 10 m. For T:H = 1, the wall falls to ≈1.5 m at 9 m, and for T:H = 2, the wall slips below unity by 9 m, signaling an unacceptable sliding risk unless a shear key or ground reinforcement is provided.

A similar trend is observed in the overturning FS (Figure 3 (b)), though the benefits of a longer heel are even more pronounced. The extended heel not only increases the stabilizing weight, but also acts at a greater lever arm from the toe. For wall heights up to 6 m, both T:H = 0.5 and 1 comfortably exceed the design requirement of FS = 1.5, while T:H = 2 approaches this threshold around 6 m and drops below it beyond 7 m. The long-heel wall (T:H = 0.5) maintained an FS greater than 3 at 7 m and about 2 at 10 m, demonstrating the effectiveness of the heel extension in resisting overturning for medium-to-tall walls. In contrast, the influence of the T:H ratio on the bearing capacity is relatively minor, especially as the wall height increases, as displayed in Figure 3 (c). At lower heights (4 m–5 m), slight differences appear, with T:H = 2 yielding marginally higher FS due to the more central position of the resultant load, which reduces the eccentricity and improves the footing stress distribution. However, as the height increases to 6–10 m, the effect of the base proportions diminishes, and the bearing FS for all cases converge and decline sharply. This indicates that, for tall walls, the bearing stability is controlled primarily by the magnitude and location of the resultant force driven by the wall height and lateral pressure rather than by the base geometry. At heights of 9 m–

10 m, the bearing FS for all T:H ratios falls to around or below the design threshold (FS = 3), making the bearing capacity the governing failure mode regardless of the base proportions. Thus, modifying the T:H ratio alone is insufficient to prevent the bearing failure in tall walls.

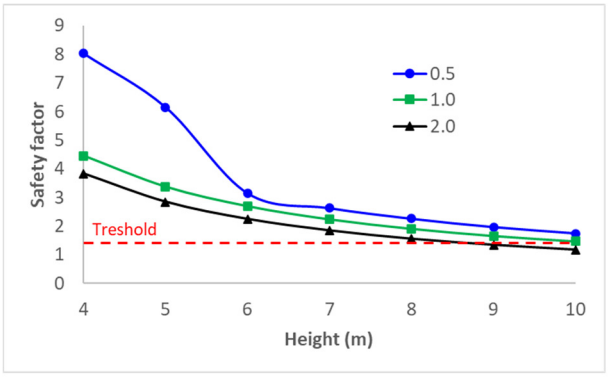

a. Sliding

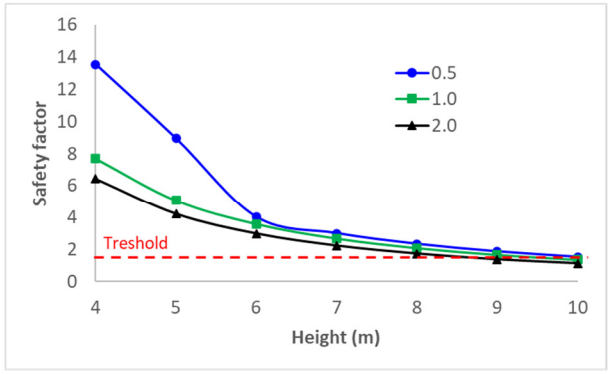

b. Overturning

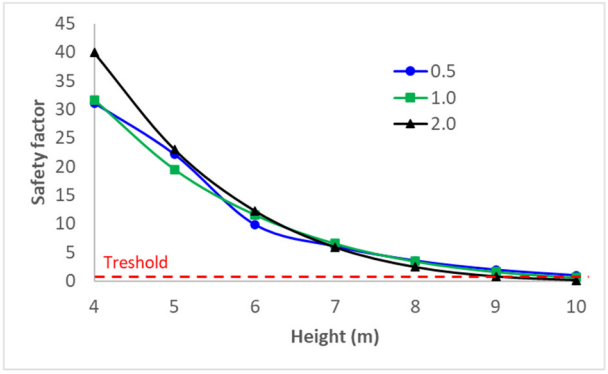

c. Bearing capacity

Fig. 3. Effect of T:H ratio on the stability of cantilever retaining walls.

Additional measures, such as widening the base, improving the foundation soil (e.g., compaction or replacement), or reducing the surcharge loads are required in such cases, particularly on weaker soils. Overall, the results show that the backfill friction angle is the dominant factor in the sliding and overturning stability, especially as the wall height increases. Low-friction backfill (ϕ = 25°) leads to significantly reduced FS beyond 6 m, while high-friction backfill (ϕ = 45°) ensures acceptable performance up to 10 m. In comparison, the variations in the T:H ratio strongly influence the sliding and overturning at low-to-medium wall heights, with T:H = 0.5 providing the best resistance due to increased stabilizing moments. However, the base geometry has little impact on the bearing capacity in tall walls, where the load magnitude and resultant force location are more critical. These findings highlight the importance of using suitable backfill materials and optimizing the base proportions during preliminary design to achieve stability across all critical modes.

IV. CONCLUSIONS

This study conducted a systematic parametric evaluation of reinforced-concrete cantilever retaining walls, focusing on two key variables: backfill friction angle (25°, 35°, 45°) and T:H ratio (0.5, 1, 2), across wall heights ranging from 4 m to 10 m under a uniform surcharge of 10 kN/m². For each configuration, Factors of Safety (FS) against sliding, overturning, and bearing-capacity failure were determined using limit-equilibrium methods. The findings address a notable gap in literature by quantifying how the soil shear strength and base geometry jointly influence the stability envelopes for practical design. The results show that increasing the backfill friction angle substantially improves the stability by reducing the active earth pressure, with the benefits being most pronounced in taller walls. The low-friction backfill (ϕ = 25°) led to premature sliding and overturning failures at heights of 6 m–7 m, while the dense granular backfill (ϕ = 45°) delayed all three limit states, extending feasible design heights to 10 m. These outcomes provide engineers with a quantitative basis for selecting backfill materials, especially in projects where the compaction control or reinforcement options are limited. The T:H ratio was most effective in enhancing the sliding and overturning resistance when the heel was extended (T:H ≈ 0.5). In contrast, longer toes (T:H ≈ 2) offered only marginal benefits at low heights and little effect at greater heights. The bearing capacity, however, was largely unaffected by the base proportions and was instead controlled by the wall height and resultant earth pressure. This challenges the common assumption that wider bases inherently improve the bearing safety, highlighting the need for supplementary measures, such as base widening or soil improvement in tall-wall applications. As this study employed a classical analytical approach without field validation or advanced numerical modeling, the results should be regarded as indicative trends under idealized conditions. Future research should incorporate Finite Element (FE) analyses or full-scale monitoring to validate the findings and better capture the soil–structure interaction effects in real-world scenarios.

ACKNOWLEDGMENT

The authors express their sincere gratitude to the Karbonara Research Institute for the invaluable support and resources provided throughout this research. Special thanks are extended to the Civil Engineering Department of BINUS University for their continuous guidance and access to the necessary facilities and equipment.

DATA AVAILABILITY

Data analysis https://zenodo.org/records/15714130.

REFERENCES

[1] S. Sharma, "Teaching Retaining Wall Design with Case Histories," *Geo-Frontiers 2011: Advances in Geotechnical Engineering*, pp. 2877–2886, Apr. 2012, https://doi.org/10.1061/41165(397)295.

[2] Q. Li, P. Li, K. Cui, Y. Ji, D. Zhang, and Y. Qing, "Seismic fragility curves for concrete gravity retaining wall," *Soil Dynamics and Earthquake Engineering*, vol. 183, Aug. 2024, Art. no. 108806, https://doi.org/10.1016/j.soildyn.2024.108806.

[3] H. Tahsin Öztürk, T. Dede, and E. Türker, "Optimum design of reinforced concrete counterfort retaining walls using TLBO, Jaya algorithm," *Structures*, vol. 25, pp. 285–296, Jun. 2020, https://doi.org/10.1016/j.istruc.2020.03.020.

[4] A. H. Gandomi and A. R. Kashani, "Automating pseudo-static analysis of concrete cantilever retaining wall using evolutionary algorithms," *Measurement*, vol. 115, pp. 104–124, Feb. 2018, https://doi.org/10.1016/j.measurement.2017.10.032.

[5] A. Diwalkar, "Analysis and Design of Retaining Wall: A Review." Social Science Research Network, Rochester, NY, Jun. 09, 2020, https://doi.org/10.2139/ssrn.3648731.

[6] F. K. Lehner and M. P. J. Schöpfer, "Slope stability and exact solutions for cohesive critical Coulomb wedges from Mohr diagrams," *Journal of Structural Geology*, vol. 116, pp. 234–240, Nov. 2018, https://doi.org/10.1016/j.jsg.2018.04.021.

[7] P. Kloukinas and G. Mylonakis, "Generalized Rankine solutions for seismic earth pressures: Validity, limitations & refinements," *Soil Dynamics and Earthquake Engineering*, vol. 179, Apr. 2024, Art. no. 108502, https://doi.org/10.1016/j.soildyn.2024.108502.

[8] B. Ukritchon, S. Chea, and S. Keawsawasvong, "Optimal design of Reinforced Concrete Cantilever Retaining Walls considering the requirement of slope stability," *KSCE Journal of Civil Engineering*, vol. 21, no. 7, pp. 2673–2682, Nov. 2017, https://doi.org/10.1007/s12205-017-1627-1.

[9] S. Talatahari and R. Sheikholeslami, "Optimum design of gravity and reinforced retaining walls using enhanced charged system search algorithm," *KSCE Journal of Civil Engineering*, vol. 18, no. 5, pp. 1464–1469, Jun. 2014, https://doi.org/10.1007/s12205-014-0406-5.

[10] B. Ding, I. Pérez-Rey, M. A. González-Fernández, S. Yuan, H. Tang, and L. R. Alejano, "Optimizing shape design in drystone retaining walls: A multi-scope approach focusing on failure mechanisms," *Construction and Building Materials*, vol. 489, Aug. 2025, Art. no. 142116, https://doi.org/10.1016/j.conbuildmat.2025.142116.

[11] Y. Pei and Y. Xia, "Design of Reinforced Cantilever Retaining Walls using Heuristic Optimization Algorithms," *Procedia Earth and Planetary Science*, vol. 5, pp. 32–36, Jan. 2012, https://doi.org/10.1016/j.proeps.2012.01.006.

[12] A. Lazizi, H. Trouzine, A. Asroun, and F. Belabdelouhab, "Numerical Simulation of Tire Reinforced Sand behind Retaining Wall Under Earthquake Excitation," *Engineering, Technology & Applied Science Research*, vol. 4, no. 2, pp. 605–611, Apr. 2014, https://doi.org/10.48084/etasr.427.

[13] E. J. Rhomberg and W. M. Street, "Optimal Design of Retaining Walls," *Journal of the Structural Division*, vol. 107, no. 5, pp. 992–1002, May 1981, https://doi.org/10.1061/JSDEAG.0005717.

[14] A. Sarıbaş and F. Erbatur, "Optimization and Sensitivity of Retaining Structures," *Journal of Geotechnical Engineering*, vol. 122, no. 8, pp. 649–656, Aug. 1996, https://doi.org/10.1061/(ASCE)0733-9410(1996)122:8(649).

[15] V. R. Greco, "Stability of Retaining Walls against Overturning," *Journal of Geotechnical and Geoenvironmental Engineering*, vol. 123, no. 8, pp. 778–780, Aug. 1997, https://doi.org/10.1061/(ASCE)1090-0241(1997)123:8(778).

[16] H. Djadouni, H. Trouzine, A. Gomes Correia, and T. F. da S. Miranda, "2D numerical analysis of a cantilever retaining wall backfilled with sand–tire chips mixtures," *European Journal of Environmental and Civil Engineering*, vol. 25, no. 6, pp. 1119–1135, Apr. 2021, https://doi.org/10.1080/19648189.2019.1570870.

[17] D. R. VandenBerge, E. C. Reed, and R. Li, "Mobilized Bearing Capacity Analysis of Global Stability for Walls Supported by Aggregate Piers," *Journal of Geotechnical and Geoenvironmental Engineering*, vol. 147, no. 6, Jun. 2021, Art. no. 04021034, https://doi.org/10.1061/(ASCE)GT.1943-5606.0002540.

[18] V. P. Singh, "Multi-Approach Global Stability Assessment of Soil Nail Walls," in *Earth Retaining Structures and Stability Analysis*, Singapore, 2023, pp. 291–301, https://doi.org/10.1007/978-981-19-7245-4_26.

[19] F. Tschuchnigg, H. F. Schweiger, S. W. Sloan, A. V. Lyamin, and I. Raissakis, "Comparison of finite-element limit analysis and strength reduction techniques," *Géotechnique*, vol. 65, no. 4, pp. 249–257, Apr. 2015, https://doi.org/10.1680/geot.14.P.022.

[20] H. F. Schweiger and F. Tschuchnigg, "A numerical study on undrained passive earth pressure," *Computers and Geotechnics*, vol. 140, Dec. 2021, Art. no. 104441, https://doi.org/10.1016/j.compgeo.2021.104441.

[21] J. Li, X. Li, M. Jing, and R. Pang, "Numerical Limit Analysis of the Stability of Reinforced Retaining Walls with the Strength Reduction Method," *Water*, vol. 14, no. 15, Jan. 2022, Art. no. 2319, https://doi.org/10.3390/w14152319.

[22] W. J. M. Rankine, "II. On the stability of loose earth," *Philosophical Transactions of the Royal Society of London*, vol. 147, pp. 9–27, Jan. 1997, https://doi.org/10.1098/rstl.1857.0003.